CALIBRATION OF THE DISCRETE ELEMENT PARAMETERS AND EXPERIMENTAL VERIFICATION OF THE OIL SUNFLOWER PLUG SEEDLING POTS
/
油葵穴盘苗钵体离散元参数标定与试验验证

Fandi ZENG[1)], Xuying LI[*1)], Hongbin BAI[1)], Ji CUI[1)], Xuening LIU[2)], Yongzhi ZHANG[1)]
[1)]Inner Mongolia Agricultural University, College of Mechanical and Electrical Engineering, Hohhot/China;
[2)] Taiyuan Agricultural Technology Extension Service Centre, Taiyuan/China
Tel: +86-0471-4309215; E-mail: zfd19508@163.com
DOI: https://doi.org/10.35633/inmateh-68-62

Keywords: *Plug seedling pot, Drop impact test, Collision impact force, Hertz-Mindlin with bonding model*

ABSTRACT
The movement of plug seedlings and the pots damage mechanism are deeply studied during the planting process, and the planting components are optimized. The Tekscan pressure distribution measurement system was used to measure the mechanical characteristics of the drop impact between the whole plug seedlings and the pots. The relative error between the collision impact force of the plug seedlings and the collision impact force of the pot is less than 20%. Therefore, a drop impact test using the pot allows the whole plug seedling to be characterized. The Hertz-Mindlin with bonding model was used to build a simulation model of the pot based on essential physical parameters. The Plackett-Burman test and the steepest climbing test determined the significant parameters and optimal intervals affecting the collision impact force: the rolling friction coefficient between the pot and pot was 0.35~0.38, the bond stiffness was 0.2~0.6 MN·m^{-3}, and the bond radius was 1.56~1.98 mm. Finally, the Box-Behnken test was performed and the quadratic regression model of the collision impact force was developed. Taking the collision impact force with a drop height of 350 mm as the target, the optimal solution is obtained: the rolling friction coefficient between the pot and pot was 0.35, the bond stiffness was 0.53 MN·m^{-3}, and bond radius 1.97 mm. The average value was used for other insignificant influence parameters. The simulation results are compared with the physical test, and the relative error is 3.65%. Therefore, the pot model established by this simulation parameter can represent the actual drop impact of the pots.

ABSTRACT
为深入研究栽植过程穴盘苗的运动规律和钵体的破损机理，进而优化栽植部件。本文采用 Tekscan 压力分布测量系统对整株穴盘苗与钵体的跌落碰撞力学特征测定，得到穴盘苗的碰撞冲击力与钵体的碰撞冲击力相对误差小于20%，可得采用钵体的掉落碰撞特性可以表征实际的穴盘苗。然后基于本征参数建立钵体的粘结模型，通过 Plackett-Burman 试验和最陡爬坡试验，确定了影响碰撞冲击力的显著性参数和最优区间：钵体-钵体的动摩擦系数为 0.35 ~0.38、粘结刚度为 0.2~0.6 MN•m^{-3} 和粘结半径为 1.56 ~1.98 mm；最终对显著性参数进行了 Box-Behnken 试验，建立了碰撞冲击力与仿真参数的二阶回归模型，并以跌落高度为 350mm 的钵体碰撞冲击力为目标进行寻优，得到最优解：钵体-钵体的动摩擦系数0.36，钵体的粘结刚度0.22 MN•m^{-3} 和粘结半径1.66 mm，相对误差为 3.65%，即采用此仿真参数建立的穴盘苗钵体模型，能表征实际穴盘苗钵体的跌落碰撞力学特性。

INTRODUCTION

Transplanting seedlings can use natural light and heat resources to improve crop quality, increase crop yield and create favourable conditions for high crop yield, which has obvious advantages in open field planting and mulch seeding *(Yang et al., 2018; Zhao et al., 2020)*. The roots of the plug seedlings are mixed and absorb the nutrients in the matrix, forming a pot with a particular strength elasticity to facilitate transplanting in the field *(Han et al., 2019; Wen et al., 2021)*. The movement of the plug seedlings and the damage mechanism of the pot is a very complex system that can seriously affect the quality and efficiency of the transplanting process.

[1] *Fandi Zeng, Ph.D. Stud. Eng;*[1]**Xuying Li, Pro. Ph.D. Eng;* [1]*Hongbin Bai, M.S. Stud. Eng.;* [1]*Ji Cui, M.S. Stud. Eng.;*
[2] *Xuening Liu, M.S. Assistant agronomist;* [1] *Yingzhi Zhang, Ph.D., Associate professor*

Many scholars have focused on research into the damage rate of plug seedlings and the optimization of critical components. *Ryu et al., (2001),* studied the effect of the structural parameters of the seedling gripper on the success of seedling extraction and the loss of quality of potted seedlings. *Jiang et al.,(2017)*, studied the effects of the matrix ratio, water content, and pot quality on seedling extraction and the matrix breakage success rate. *Yang et al., (1991)*, studied the influencing factors of the operational performance of the sliding needle cylinder seedling gripper and analysed the influence of the degree of disc root and the water content of the matrix on the success rate of seedling extraction. *Mao et al., (2021)*, designed a seedling pickup device composed mainly of a conveying device, a feeding device, a seedling clamping device, and an automatic control system. The use of aerodynamically blowing out the seedlings and the end effector significantly reduces the damage rate of the seedlings. *Tian et al., (2022)*, modelled matrix particles of different materials based on the elastic-plastic contact model (ECM) in EDEM to study the interaction between the steel needle and the matrix. Using the response surface method, we investigate changes in matrix loss with different needle diameters, insertion depths, and insertion and grasping speeds. *Liu et al., (2016)*, established a mechanical model for the stage of seedling taking and planting. Combined with the test of the pressure resistance characteristics of the pot, the relevant parameters of the pot suitable for mechanized transplanting were obtained. According to *Jin et al., (2018)*, the high-speed photographic analysis of the collision movement process of the planting device and the seedlings falling to the bottom of the planter established the dynamic model of each stage. *Gao et al., (2017)*, established seedling matrix particle models of various materials based on the extracellular cohesion matrix (ECM) cohesion model and then studied the relationship between the steel needle and the seedling matrix. It is not easy to accurately describe the movement of plug seedlings and pot damage by conventional methods. The discrete element method considers the influence and distribution of physical parameters on particle flow. The velocity and displacement of each particle are solved by Newton's second law and the dynamic relaxation method *(Han et al., 2019; González-Montellano et al., 2012)*. It is especially suitable for studying nonlinear problems such as the pot damage mechanism.

Because there is a multidirectional and complex force chain network between the particles of the pots, it is necessary to input exact simulation parameters to obtain accurate simulation results. At present, individual parameters are mainly measured, but rarely are the parameters of the pot measured in a more comprehensive physical test. In this study, T562 oilseed sunflower plug seedlings were used to study the mechanical characteristics of the drop impact of the whole plug seedling and the pot using the Tekscan pressure distribution measurement system. The Hertz-Mindlin with bonding model was used to build a simulation model of the pot based on essential physical parameters. Taking the collision impact force with a drop height of 350 mm as the target, the PB, steep climb, and Box-Behnken tests were carried out to calibrate the simulation parameters. Simulated collision impact forces are compared with actual collision impact forces to verify the reliability of the model. This study provides a basis for studying the movement of plug seedlings and the pot damage mechanism.

MATERIALS AND METHODS

Test material

In this test, T562 oil sunflower plug seedlings were grown by Inner Mongolia Heyuan Agricultural Technology Corporation. The seedling matrix consisted of grass carbon, vermiculite, and pearlstone with a mass ratio of 3:1:1 *(Zeng et al., 2021)*. The age of the seedlings was 30 d. The water content was 58.78~62.47% by the drying method. The oil sunflower seedlings grew normally, with well-developed root systems knotted together with the seedling matrix to form a strong and flexible pot, as shown in Figure 1.

Fig. 1 – Oil sunflower plug seedlings at the planting stage

Physical test of drop impact between the pots and the whole plug seedlings

As shown in Figure 2, the drop impact test between the plug seedling and the steel plate is composed mainly of a seedling gripper, frame, handle, 5250 flexible thin film network tactile pressure sensor, and computer. The 5250 flexible thin film network tactile pressure sensor, handle, and I-Scan System data processing system make up the Tekscan pressure distribution measurement system *(Hunston, 2002)*. The flexible thin film network tactile pressure sensor is a matrix-based thin film pressure sensor consisting of 2 very thin polyester films. The sensor size is 245.9×245.9 mm, the spatial resolution is 3.2/cm^2, the pressure measurement range is 0~0.179 MPa, and the scanning frequency is 0~100 Hz, as shown in Figure 3. A flexible thin film network tactile pressure sensor was placed at the centre of the seedling gripper for testing *(Agins et al., 2003; Yang et al., 2016)*. During the test, the flexible thin film network tactile pressure sensor sweeps each sensing point and then measures the pressure resistance of each force sensing point. Numerical analysis is performed to convert data on contact stress, contact area, and peak contact stress and generate the corresponding distribution clouds *(Chevalier et al., 2010; Mei, 2021)*.

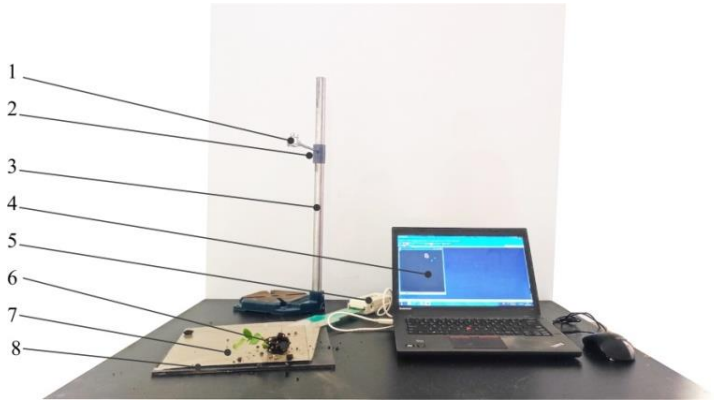

Fig. 2 – Drop impact test on oil sunflower plug seedlings

1. Seedling gripper. 2. Fastening bolts. 3. Frame. 4. Computer and I-Scan System data processing system. 5. Handle. 6. Plug seedlings. 7. 5250 flexible thin film network tactile pressure sensor. 8. The steel plate.

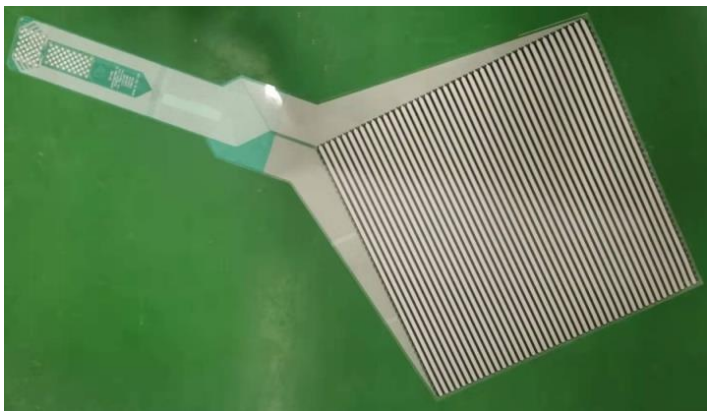

Fig. 3 – 5250 flexible thin film network tactile pressure sensor

The sensor should be calibrated and zeroed before the test. The whole plug seedlings and the pots are dropped against the steel plate at different heights. The steel has a density of 7850 kg/m^3, a Poisson's ratio of 0.3, a shear modulus of 7.0 x 10^{10} Pa, and a thickness of 5 mm. The drop height (*h*) is the distance from the bottom of the pot to the test plane (Figure 4a).

The test is divided into two main cases, as shown in Figure 4. A steel plate is placed on the test plane, a flexible film network tactile pressure sensor is arranged on it, and the drop impact test of the plug seedling at different drop heights is carried out; The collision between the pot and the steel plate retains the 20 mm stem above the pot so that the seedling gripper can hold the pot. The pots carried out drop impact at different drop heights. This process was repeated in each group several times, and the final value of the average was calculated.

(a) (b)

Fig. 4 – Comparison of whole plug seedlings and pots

a) holding position of the plug seedling; b) whole plug seedling and pot

Determination of the basic parameters of the pot

The mass, density, and other essential parameters of the pot of the T562 oil sunflower plug seedlings are shown in Table 1.

Table 1

Basic physical parameters of the pots

Parameters	Value
Physical dimensions(Top surface × Bottom surface × Height) [mm×mm×mm]	40×20×45
The pot volume [cm^3]	42
Mass [g]	15
Density [kg/m^3]	357

Determination of the restitution coefficient

The restitution coefficient measures the ability of a plug seedling to recover its original shape after a collision and is an essential parameter for analysing changes in the movement of plug seedlings *(Ma et al., 2020)*.The free-falling collision method determined the restitution coefficient of collision between the pot and the steel plate. When the pot falls onto the steel plate, the restitution coefficient *e* is the ratio of the relative velocity of the pot to the steel plate after the collision to the relative velocity before the collision.

$$e= v_2/v_1 \quad (1)$$

Where v_1 and v_2 are the velocities of the pot before and after the collision, m/s.

The pot is under the action of gravity during the falling process. The kinetic energy theorem obtains the normal velocity of the pot before the collision.

$$v_1=\sqrt{2gh_1} \quad (2)$$

Normal velocity after collision:

$$v_2=\sqrt{2gh_2} \quad (3)$$

Therefore,

$$e=\frac{|v_2|}{|v_1|}=\sqrt{\frac{h_2}{h_1}} \quad (4)$$

where v_2 is the normal velocity before the collision, m/s; v_1 is the normal velocity after the collision, m/s; h_1 is the drop height before the collision, mm; and h_2 is the maximum height of the bounce after the collision, mm.

The pots with well-wrapped roots were selected for marking to facilitate the high-speed camera shooting, collision, and rebound effect. The distance between the high-speed camera lens and the test surface was 2000 mm. The marker point of the plug seedling pot fell freely from a height of 350 mm to the steel plate collision and bounced up.

Determination of the restitution coefficient

As shown in Figure 5, the CNY-1 type inclinometer was placed on the horizontal plane *(Zhang et al., 2018)*. The pot was broken up and placed in the cylindrical container to form the cylindrical pot block. The lower surface of the cylindrical container bonded to the test plane of the inclinometer. The inclinometer was turned anticlockwise until the pot was seen to slide. The rotation was stopped, and the angle of the inclination display was recorded at this point.

The static friction coefficient between the pot and pot was calculated from Equation 5. This process was repeated in each group several times, and the final value of the average was calculated. Therefore, the static friction coefficient between the pot and pot is 0.75~0.92; the static friction coefficient between the pot and steel is 0.7~0.88.

$$\mu = \tan \varphi \quad (5)$$

where: μ is the static friction coefficient, and φ is the angle indicated when the pot is about to slide in the plane of determination of the inclinometer, (°).

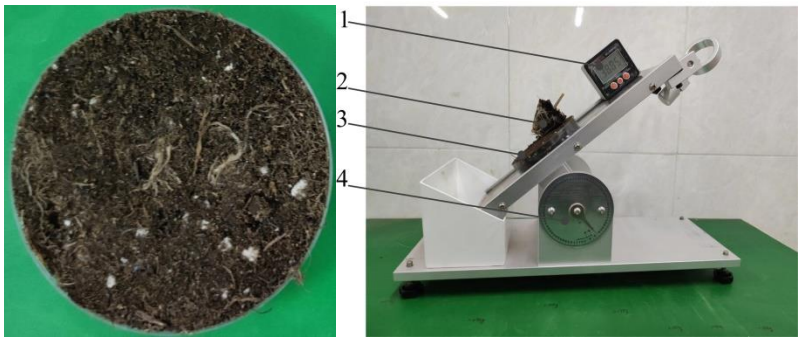

Fig. 5 – Static friction coefficient test between the pot and pot
a) cylindrical pot block; b) static friction coefficient test device

Establishment of the pot contact model

The geometric characteristics of the particles are irregular in the pot, with small holes forming between the particles. The position of the pot particles changes when the pot collides with a vital component of the transplanter *(Ma et al., 2021; Wang, 2016)*. The Hertz-Mindlin with bonding model was chosen as the contact model between the pot's movement and the damage mechanism. In this paper, spherical particles were used as the base particles for the pot model. The particle radius is set to 1.3 mm. The total number of particles was 2587, and the bonding bonds were 42027. The time step was 1%. The data storage time interval is 0.0001 s. The total movement time was 1.6 s. A physical and discrete element simulation model of the plug seedling pot is shown in Figure 6.

Fig. 6 – Physical and discrete element simulation model of the pot

The Hertz-Mindlin with bonding model is based on 5 microscopic parameters: normal bond stiffness S_n, tangential bond stiffness S_t, normal ultimate stress σ_{max}, tangential ultimate stress τ_{max}, and bond radius R_b *(Xiong et al., 2018; Zhang et al., 2019)*. To improve the efficiency of the operation, the bond stiffness and ultimate stress of the pot particles are equal so that $S_n = S_t$ and $\sigma_{max} = \tau_{max}$. The bond radius R_b is usually 1.2~2 times the radius of the particle. Through many drop impact simulations, the initial ranges of the parameters of the discrete element model of the pot, including the bond stiffness, ultimate stress, and bond radius, are 0.2-1.2 MN·m^{-3}, 0.06-0.16 MPa, and 1.56-2.60 mm.

Establishment of the discrete element model of the pot drop impact

First, a discrete element model of dropping impact between the pot and the steel plate was established based on the physical test. Then, the pot particle coordinates were copied into the particle factory data file "Particle_Cluster_Data.txt." The basic information about the pot particles was written into "Particle Replacement prefs.txt." Import the API file "Particlereplacement_v2_x64.dll" with the particle factory into EDEM 2018.

Finally, the parameters were set according to the relevant test scheme, and a simulation was carried out. The discrete element model of the collision between the pot and the steel plate is shown in Figure 7.

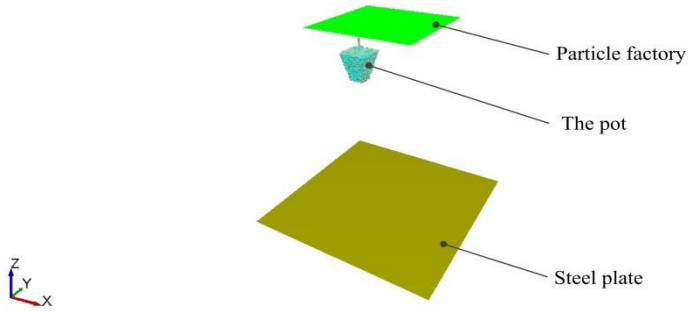

Fig. 7 – Discrete element model of the pot drop impact

RESULTS

Determination of collision impact mechanics between the whole plug seedling and the pot

Analysis of the contact stress distribution characteristics between the whole plug seedling and the pot

The whole oil sunflower plug seedlings and pots were subjected to drop impact tests at different heights. The flexible film network tactile pressure sensor and the I-Scan System data processing system obtained the contact stress and its distribution of the collision between the whole seedling and the pot, as shown in Figure 8. The dark blue area is low stress, the red area is high stress, and the colourless area has a contact stress of 0 kPa. The high stress is located approximately in the centre of the contact area, and the stress values decrease from the centre to the edge of the contact area. As the drop height increases, the low-stress distribution decreases significantly. It is gradually distributed toward the edge of the contact area, while the high-stress distribution gradually increases.

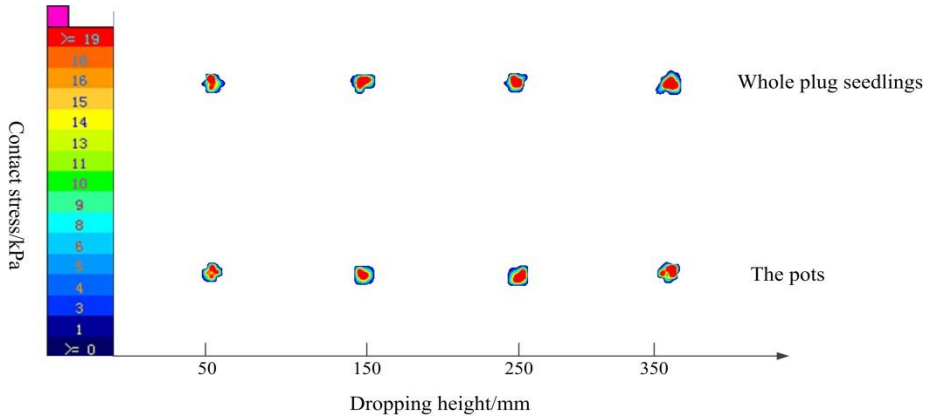

Fig. 8 – Typical stress distribution of dropping impact between whole plug seedlings and the pots

Comparing the collision impact force of the whole plug seedlings and the pots

The I-Scan System is used to process the data to obtain the average contact stress and contact area for a drop impact of an oil sunflower plug seedling. The product of the average contact stress (P) and the contact area (A) is the collision impact force *(Wu et al., 2012)*, as shown in Equation (6).

$$F=P\times A\times 10^{-3} \quad (6)$$

where F is the collision impact force, N; A is the contact area, mm^2; and P is the average contact stress, kPa.

As shown in Table 2, the relative error between the collision impact force of the plug seedlings and the collision impact force of the pot is less than 20%. Therefore, a drop impact test using the pot allows the whole plug seedling to be characterized. It provides support for the discrete element simulation.

Table 2

Comparison of collision impact forces

Type	Dropping height/mm			
	50 mm	150 mm	250 mm	350 mm
Collision impact force of the whole seedlings[N]	4.63	5.37	6.39	7.68
Collision impact force of the pot[N]	3.95	4.75	5.64	6.84
Relative error[%]	14.69	11.55	11.74	10.94

Restitution coefficient test results

The collision process of the pot was recorded with a PCO.dimax S4 high-speed camera. The distance in the horizontal direction is 400 mm, and the displacement in the vertical direction is 700 mm in the image post-processing software TEMA. The vertical displacement curve is shown in Figure 9.

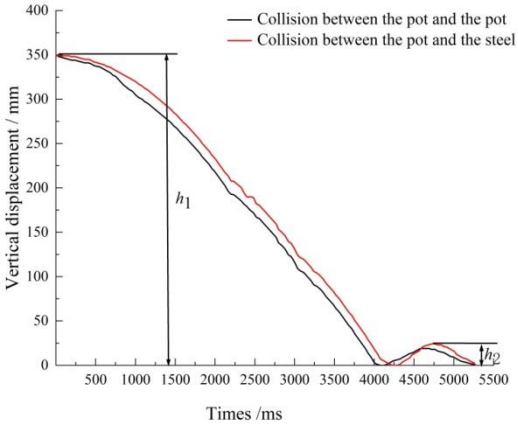

Fig. 9 – Vertical displacement curve

This process was repeated in each group several times, and the final value of the average was calculated. The restitution coefficient between the pot and the pot is 0.26~0.48; the restitution coefficient between the pot and the steel is 0.17~0.24.

Significance parameter selection and analysis of results

The Plackett-Burman experimental design was carried out using Design-Expert 8.0.6 software. The restitution coefficient between the pot and the pot, and the friction coefficient between the pot and steel were determined by high-speed photography and an inclinometer. Additional parameters were consulted in the relevant literature *(Cui et al., 2022; Feng, 2016; Gao, Xie, et al., 2017; Tong et al., 2019)*. A Plackett-Burman test was conducted to identify the parameters that would have significant effect on the collision impact force. Respectively, the maximum and minimum values of the 11 parameters were coded as levels +1 and -1 in Table 3. A total of 12 sets of tests were carried out, with each set being averaged several times to determine the collision impact force. The Plackett-Burman test design and results are shown in Table 4.

Table 3

The Placket - Burman test parameters table

No.	Test parameters	Low level (-1)	High level (+1)
X_1	Poisson's ratio of the pot	0.3	0.44
X_2	Shear strength of the pot [MPa]	1.04	1.76
X_3	the restitution coefficient between the pot and the pot	0.26	0.48
X_4	the static friction coefficient between the pot and pot	0.75	0.92
X_5	the rolling friction coefficient between the pot and pot	0.35	0.43
X_6	the restitution coefficient between the pot and the steel	0.17	0.24
X_7	the static friction coefficient between the pot and steel	0.7	0.88
X_8	the rolling friction coefficient between the pot and steel	0.26	0.3
X_9	Bond stiffness[MN·m^{-3}]	0.2	1.2
X_{10}	Ultimate stress[MPa]	0.06	0.16
X_{11}	Bonding radius[mm]	1.56	2.6

Table 4

The Placket - Burman test design and results

No.	X_1	X_2	X_3	X_4	X_5	X_6	X_7	X_8	X_9	X_{10}	X_{11}	Collision impact force [N]
1	1	1	-1	1	1	1	-1	-1	-1	1	-1	5.39
2	-1	-1	-1	1	-1	1	1	-1	1	1	1	15.11
3	-1	1	1	1	-1	-1	-1	1	-1	1	1	9.86

4	1	1	-1	-1	-1	1	-1	1	1	-1	1	18.14
5	1	-1	1	1	-1	1	1	1	-1	-1	-1	6.33
6	1	-1	1	1	1	-1	-1	-1	1	-1	1	13.7
7	1	-1	-1	-1	1	-1	1	1	-1	1	1	10.91
8	-1	-1	-1	-1	-1	-1	-1	-1	-1	-1	-1	5.82
9	-1	-1	1	-1	1	1	-1	1	1	1	-1	6.38
10	1	1	1	-1	-1	-1	1	-1	1	1	-1	11.54
11	-1	1	1	-1	1	1	1	-1	-1	-1	1	4.35
12	-1	1	-1	1	1	-1	1	1	1	-1	-1	6.99

Determination of the optimal interval

As shown in Table 5, the rolling friction coefficient between the pot and pot (X_5), bond stiffness (X_9), and bond radius (X_{11}) have a significant effect on the collision impact force of the pot. Therefore the steepest climb test was carried out for parameters X_5, X_9, and X_{11}. To further limit the range of parameter values, the relative error between the simulated collision impact force and collision impact force obtained from the physical test (F=6.84 N) was used as the evaluation index, and the average value was used for all insignificant influence parameters. The design and the result of the steepest climb test are shown in Table 6. The results showed that the rolling friction coefficient between the pot and pot (X_5) was 0.35~0.38, the bond stiffness (X_9) was 0.2~0.6 MN·m^{-3}, and the bond radius (X_{11}) was 1.56~1.98 mm.

Table 5

Placket - Burman parameters significant analysis

Parameters	Stdized effect	Sum of Square	Contribution rate/%	Significance ranking
X_1	2.92	25.52	11.98	4
X_2	-0.33	0.33	0.15	10
X_3	-1.7	8.67	4.07	5
X_4	0.04	0.0047	0.002253	11
X_5	-3.18	30.34	14.24	3
X_6	-0.52	0.81	0.38	8
X_7	-0.68	1.37	0.64	6
X_8	0.45	0.61	0.29	9
X_9	4.87	71.05	33.35	2
X_{10}	0.64	1.24	0.58	7
X_{11}	4.94	73.11	34.32	1

Table 6

The test design scheme and results of the steepest climb

No.	Parameters X_5	Parameters X_9	Parameters X_{11}	Collision impact force	Relative error
	[-]	[MN·m^{-3}]	[mm]	[N]	[%]
1	0.35	0.2	1.56	5.81	15.06
2	0.37	0.4	1.77	7.67	12.13
3	0.38	0.6	1.98	9.08	32.75
4	0.40	0.8	2.19	13.32	94.74
5	0.41	1.0	2.40	10.86	58.77
6	0.43	1.2	2.60	8.73	27.63

Collision impact force-simulation parameter regression model establishment

The rolling friction coefficient between the pot and pot X_5, bond stiffness X_9 and bond radius X_{11} were used as test factors. The collision impact force is the response value, and the Box-Behnken module is used to design a 3-factor, 3-level orthogonal test. The test factors and levels are shown in Table 7. A total of 17 tests were carried out and repeated in each group multiple times, and the final value was the average.

Table 7

Test factors and levels

Factors	The level of coding		
	-1	0	+1
The rolling friction coefficient between the pot and pot X_5	0.35	0.37	0.38
Bond stiffness X_9[MN·m^{-3}]	0.2	0.4	0.6
Bonding radius X_{11}[mm]	1.56	1.77	1.98

As shown in Table 8, Design-Expert 8.0.6 software was used to perform multiple regression analyses on the test results of the collision impact force. A quadratic regression model of the rolling friction coefficient between the pot and pot (X_5), bond stiffness (X_9), and bond radius (X_{11}) was established, as shown in Equation 7.

$$\begin{cases} F=9.52-0.57\times X_5+0.45\times X_9-0.40\times X_{11}+2.13\times X_5X_9+ \\ 1.82\times X_5X_{11}-1.51\times X_9X_{11}+1.81\times X_5^2-1.17\times X_9^2-0.44\times X_{11}^2 \end{cases} \quad (7)$$

where:

F is the collision impact force, N; X_5, X_9, and X_{11} are the rolling friction coefficients between the pot and pot, bond stiffness (MN·m^{-3}) and bond radius (mm), respectively.

Table 8

Box-Behnken test design and results

No.	Test factor level value			Collision impact force
	X_5	X_9	X_{11}	[N]
1	0	0	0	9.68
2	-1	0	1	9.67
3	1	-1	0	6.82
4	0	-1	1	8.62
5	-1	0	-1	13.53
6	-1	-1	0	11.97
7	0	-1	-1	6.99
8	0	1	-1	10.24
9	1	0	1	11.92
10	-1	1	0	9.26
11	0	0	0	9.53
12	0	0	0	9.87
13	1	0	-1	8.49
14	0	0	0	9.46
15	0	0	0	9.08
16	1	1	0	12.64
17	0	1	1	5.84

The analysis of variance (ANOVA) results for the above quadratic regression model of collision impact force. The coefficient of determination of the regression Equation R^2=0.9699 and the corrected coefficient of determination adjusted R^2=0.9312 are close to 1, and the coefficient of variation CV=5.60%, so the confidence level of the obtained regression equation is high. The lack of fit P=0.051>0.05 indicates that the regression equation fits well and can better reflect the relationship between collision impact force F and X_5, X_9, and X_{11}.

Table 9

The analysis of variance (ANOVA) on the collision impact force model

Source	Sum of Squares	Freedom	Mean Square	*F* Value	*P* value
Model	65.42	9	7.27	25.05	0.0002**
X_5	2.6	1	2.6	8.96	0.0201*
X_9	1.6	1	1.6	5.52	0.0511
X_{11}	1.28	1	1.28	4.41	0.0738
X_5 X_9	18.19	1	18.19	62.69	<0.0001**
X_5 X_{11}	13.29	1	13.29	45.79	0.0003**
X_9 X_{11}	9.09	1	9.09	31.33	0.0008**
X_5^2	13.86	1	13.86	47.77	0.0002**
X_9^2	5.72	1	5.72	19.72	0.003**
X_{11}^2	0.8	1	0.8	2.76	0.1409
Residual	2.03	7	0.29		
Lack of Fit	1.69	3	0.56	6.51	0.051
Pure Error	0.35	4	0.086		
Cor Total	67.45	16			

*Note: * indicates significant (p<0.05), ** indicates highly significant (p<0.01)*

Selection and verification of optimal parameters

With the optimization module of Design-Expert 8.0.6 software, the collision impact force (*F*=6.84 N) of the physical test measured drop height of 350 mm was used as the target. The software calculated the optimal solution: the rolling friction coefficient between the pot and pot was 0.35, the bond stiffness was 0.53 MN·m^{-3}, and bond radius 1.97 mm. The average value was used for other insignificant influence parameters. The Poisson's ratio was 0.37, and the shear modulus was 1.4 MPa. The restitution coefficient between the pot and the pot was 0.37. The static friction coefficient between the pot and the pot was 0.84, the restitution coefficient between the pot and the steel was 0.21, the static friction coefficient between the pot and the steel was 0.79, the rolling friction coefficient between the pot and steel was 0.28, and the ultimate stress was 0.11MPa. The simulation results are compared with the physical test, and the relative error is 3.65%. Therefore, the pot model established by this simulation parameter can represent the actual drop impact of the pots.

CONCLUSIONS

(i) The Tekscan pressure distribution measurement system was used to measure the mechanical characteristics of the drop impact between the whole plug seedlings and the pots. The relative error between the collision impact force of the plug seedlings and the collision impact force of the pots is less than 20%.

(ii) The Plackett-Burman test and the steepest climbing test determined the significant parameters and optimal intervals affecting the collision impact force: the rolling friction coefficient between the pot and pot was 0.35~0.38, the bond stiffness was 0.2~0.6 MN·m^{-3}, and the bond radius was 1.56~1.98 mm.

(iii) The Box-Behnken test was performed on the significance of the parameters, and the quadratic regression model of the collision impact force was developed. Taking the collision impact force with a drop height of 350 mm as the target, the optimal solution was obtained: the rolling friction coefficient between the pot and pot was 0.35, the bond stiffness was 0.53 MN·m^{-3}, and bond radius was 1.97 mm. The average value was used for other insignificant influence parameters. The simulation results were compared with the physical test, and the relative error was 3.65%. Therefore, the pot model established by this simulation parameter can represent the actual drop impact of the pots.

ACKNOWLEDGEMENT

This project was funded by National Natural Science Foundation of China (NSFC) (32160423) and the Natural Science Foundation of the Inner Mongolia Autonomous Region of China (2020MS05055).

REFERENCES

[1] Yang, Q. Z., Xu, L., Shi, X. Y., Ibrar, A., Mao, H. P., Hu, J. P., & Han, L. H. (2018). Design of seedlings separation device with reciprocating movement seedling cups and its controlling system of the full-automatic plug seedling transplanter. *Computers and Electronics in Agriculture, 147*, 131-145. https://doi.org/10.1016/j.compag.2018.02.004

[2] Zhao, X., Zhang, X. S., Wu, Q. P., Dai, L., & Chen, J. N. (2020). Research and experiment of a novel flower transplanting device using hybrid-driven mechanism. *International Journal of Agricultural and Biological Engineering, 13*(2), 92-100. https://doi.org/10.25165/j.ijabe.20201302.5187

[3] Han, L. H., Francis, K., Mao, H. P., & Hu, J. P. (2019). Design and tests of a multi-pin flexible seedling pick-up gripper for automatic transplanting. *Applied Engineering in Agriculture, 35*(6), 949-957. https://doi.org/10.13031/aea.13426

[4] Wen, Y. S., Zhang, L. A., Huang, X. M., Yuan, T., Zhang, J., Tan, Y., & Feng, Z. (2021). Design of and experiment with seedling selection system for automatic transplanter for vegetable plug seedlings. *Agronomy, 11*(10), 2031.

[5] Ryu, K. H., Kim, G. Y., & Lee, H. H. (2001). Development of a robotic transplanter for bedding plants *Journal of Agricultural Engineering Research, 78*(2), 141-146.

[6] Jiang, Z. H., Hu, Y., Jiang, H. Y., & Tong, J. H. (2017). Design and force analysis of end-effector for plug seedling transplanter. *Plos One, 12*(7), 1-15.

[7] Yang, Ting, K. C., & Giacomelli, G. A. (1991). Factors affecting performance of sliding-needles gripper during robotic transplanting of seedlings. *Applied Engineering in Agriculture, 7*(4), 493-498.

[8] Mao, H. P., Ma, G. X., Han, L. H., Jian, P. H., Gao, F., & Liu, Y. (2021). A whole row automatic pick-up device using air force to blow out vegetable plug seedlings. *Spanish Journal of Agricultural Research, 18*(4). https://doi.org/10.5424/sjar/2020184-17003

[9] Tian, Z. W., Ma, W., Yang, Q. C., Yao, S., Guo, X. Y., & Duan, F. M. (2022). Design and experiment of gripper for greenhouse plug seedling transplanting based on EDM. *Agronomy, 12*(7). https://doi.org/10.3390/agronomy12071487

[10] Liu, J. D., Cao, W. B., Tian, D. Y., Ouyang, Y. N., & Zhao, H. Z. (2016). Optimization experiment of transplanting actuator parameters based on mechanical property of seedling pot（基于苗钵力学特性的自动移栽机执行机构参数优化试验）. *Transactions of the CSAE, 32*(16), 32-39.

[11] Jin, X., Ji, J. T., Liu, W. X., He, Y. K., & Wu, D. X. (2018). Structural optimization of duckbilled transplanter based on dynamic model of pot seedling movement（基于钵苗运动动力学模型的鸭嘴式移栽机结构优化）. *Transactions of the CSAE, 34*(09), 58-67.

[12] Gao, G. H., Wang, K., & Sun, X. N. (2017). Verification for EDEM simulation of process of jacking tray-seedling by steel needle in grafting machine and parameter optimization（嫁接机钢针顶起穴盘苗过程EDEM模拟验证及参数优化）. *Transactions of the CSAE, 33*(21), 29-35.

[13] Han, B., Shen, D. S., Guo, C., Liu, Q., Wang, X., & Song, C. B. (2019). Design and experiment of adjustable end-effector of cabbage seedlings（可调节式甘蓝钵苗取苗末端执行器设计与试验）. *Transactions of the CSAM, 50*(11), 111-120.

[14] González-Montellano, C., Fuentes, J. M., Ayuga-Téllez, E., & Ayuga, F. (2012). Determination of the mechanical properties of maize grains and olives required for use in DEM simulations. *Journal of food engineering, 111*(4), 553-562. https://doi.org/10.1016/j.jfoodeng.2012.03.017

[15] Zeng, F. D., Li, X. Y., Li, X., Su, Q., & Zhang, Y. Z. (2021). Experiment and analysis of high-speed photographic techniques for throwing motion of seedlings（基于高速摄影技术穴盘苗抛投运动试验与分析）. *Journal of China Agricultural University, 26*(09), 168-176.

[16] Hunston, M. (2002). Innovative thin-film pressure mapping sensors. *Sensor Review, 22*(4), 319-321.

[17] Agins, H. J., Harder, V. S., Lautenschlager, E. P., & Kudrna, J. C. (2003). Effects of sterilization on the Tekscan digital pressure sensor. *Med Eng Phys, 25*(9), 775-780. https://doi.org/10.1016/s1350-4533(03)00119-x

[18] Yang, L. J., Zhang, Y., Liu, D. H., Xu, B. P., & Liu, C. X. (2016). Early recognition for dairy cow lameness based on pressure distribution measurement system（基于压力分布测量系统的奶牛跛行早期识别）. *Transactions of the CSAM, 47*(S1), 426-432.

[19] Chevalier, T. L., Hodgins, H., & Chockalingam, N. (2010). Plantar pressure measurements using an in-shoe system and a pressure platform: a comparison. *Gait Posture, 31*(3), 397-399. https://doi.org/10.1016/j.gaitpost.2009.11.016

[20] Mei, Y. (2021). *Research on the bionic mechanism and coupled bionic design method of green tire pattern structure* [Doctor's thesis], Jiang Su University.

[21] Ma, Y. H., Song, C. D., Xuan, C. Z., Wang, H. Y., Yang, S., & Wu, P. (2020). Parameters calibration of discrete element model for alfalfa straw compression simulation（苜蓿秸秆压缩仿真离散元模型参数标定）. *Transactions of the CSAE, 36*(11), 22-30.

[22] Zhang, T., Liu, F., Zhao, M. Q., Ma, Q., Wei, W., Qi, F., & Peng, Y. (2018). Determination of corn stalk contact parameters and calibration of discrete element simulation（玉米秸秆接触物理参数测定与离散元仿真标定）. *Journal of China Agricultural University, 23*(04), 120-127.

[23] Ma, G. X. (2021). *Study on enhancement mechanism of low loss seedling picking in biochar and air ejection-package clamping pick-up device* [Doctor's thesis], JiangSu University.

[24] Wang, Y. Y. (2016). *Key technologies of vegetable plug seedlings transplanting based on machine vision and simulation test* [Ph.D. dissertation Doctor's thesis], Jilin University.

[25] Xiong, P. Y., Yang, Z., Sun, Z. Q., Zhang, Q. Q., Qing, H. Y., & Wei, Z. Z. (2018). Simulation analysis and experiment for three-axis working resistances of rotary blade based on discrete element method（基于离散元法的旋耕刀三向工作阻力仿真分析与试验）. *Transactions of the CSAE, 34*(18), 113-121.

[26] Zhang, L. F., Song, X. F., Zhang, X. K., Zhang, F. Y., Cheng, W. W., & Fei, D. (2019). Simulation and experiment on mechanical characteristics of kneading and crushing process of corn straw（玉米秸秆揉丝破碎过程力学特性仿真与试验）. *Transactions of the CSAE, 35*(09), 58-65.

[27] Wu, J., Guo, K. Q., Ge, Y., & Wang, Y. Y. (2012). Contact pressure distribution characteristics of Korla pear fruit at moment of drop impact（香梨果实跌落碰撞时的接触应力分布特性）. *Transactions of the CSAE, 28*(01), 250-254+300.

[28] Cui, Y. J., Wei, Y. Z., Ding, X. T., Cui, G. P., He, Z., & Wang, M. H. (2022). Design and experiment of adjustable spacing end-effector based on cylindrical cam（基于圆柱凸轮的株距可调式取苗末端执行器设计与试验）. *Transactions of the CSAM, 53*(01), 104-114+122.

[29] Feng, T. X. (2016). *Optimization design and test research of plug seedings end-effector in greenhouse* [Master's thesis], Beijing University of Technology.

[30] Gao, G. H., Xie, H. F., & Wang, T. B. (2017). EDEM simulation and experiment of pullout force of protected vegetable harvester（设施蔬菜收获机拉拔力学性能 EDEM 仿真与试验）. *Transactions of the CSAE, 33*(23), 24-31.

[31] Tong, J. H., Shi, H. F., Wu, C. Y., Ding, Y. H., Zhao, X., & Wang, R. Y. (2019). Simulation and test of seedling pot grabbing by spade end-effector（穴盘移栽指铲式末端执行器苗钵基质抓取仿真与试验）. *Transactions of the CSAM, 50*(08), 107-116.